

Progress Toward Generation of Spatially-Entangled Photon Pairs in a Few-Mode Fiber

Afshin Shamsschooli
Dept. of Electrical Engineering
University of Texas at Arlington
Arlington, TX, USA
afshin.shamsschooli@mavs.uta.edu

Cheng Guo
Dept. of Electrical Engineering
University of Texas at Arlington
Arlington, TX, USA
cheng.guo@mavs.uta.edu

Michael Vasilyev
Dept. of Electrical Engineering
University of Texas at Arlington
Arlington, TX, USA
vasilyev@uta.edu

Francesca Parmigiani
Microsoft Research
Cambridge, CB1 2FB, UK
Francesca Parmigiani
Francesca.Parmigiani@microsoft.com

Xiaoying Li
College of Precision Instruments and Opto-
electronics Engineering, Tianjin University
Tianjin, 300072, China
xiaoyingli@tju.edu.cn

Abstract—Aiming at producing spatial-mode-entangled photon pairs in a few-mode fiber, we experimentally demonstrate generation of idler beam from a seed signal in a superposition of two fiber modes. For every signal mode superposition, we observe the indication of idler mode orthogonality to the signal mode.

Keywords—Nonlinear optics in fibers, inter-modal four-wave mixing, quantum information processing.

I. INTRODUCTION

Entanglement in multiple degrees of freedom, e.g., in polarization, frequency, time-bin, and spatial modes has a potential for carrying larger amounts of quantum information, which is important for quantum communication and information processing. While polarization, frequency, and time-bin entanglement generation has already been implemented in integrated form compatible with low-loss transport over optical fiber, the spatial entanglement still relies on bulk-crystal-based setups, e.g., spatially- or orbital-angular-momentum- (OAM) entangled photons have been generated in crystal platforms and transported over hollow-core photonic crystal fiber [1], a few-mode fiber (FMF) [2], and vortex fiber [3]. As a possible alternative to crystal platform, FMF is gaining traction for nonlinear devices based on inter-modal four-wave mixing (IM-FWM), owing to FMF's wide options for mode- and dispersion-engineering, and excellent mode match to the FMFs used in low-loss transmission links. Correlated photon pairs were recently generated in FMFs by IM-FWM [4, 5], but no attempts of spatial-mode entanglement have been made yet. We have recently described a novel scheme for generation of spatial-mode-entangled photon pairs directly in the FMF using a combination of two IM-FWM processes [6]. Using classical seed signals, we experimentally measured signal-idler mode selectivity separately for these two processes. In this paper, we further combine both processes and observe that they couple the input two-mode seed signal to an orthogonal two-mode idler for various signal-mode superpositions.

Our spatial-mode entanglement scheme employs a combination of two IM-FWM processes of Fig. 1a. We use an elliptical-core FMF [7] that supports three non-degenerate modes: LP_{01} , LP_{11a} , and LP_{11b} , to be referred to as three-mode fiber (TMF) below. In IM-FWM process 1, with the help of pumps 1 and 2 a signal photon is created in mode LP_{01} at frequency ν_s , while idler photon is created in mode LP_{11a} at frequency ν_i . In process 2, their roles interchange: in the presence of pumps 3 and 4, signal photon at frequency ν_s is created in mode LP_{11a} , whereas the idler photon at frequency ν_i is created in mode LP_{01} . With all 4 pumps present, both processes occur simultaneously. Their probabilities can be equalized by adjusting relative powers of the two pump pairs, which leads to generating the maximally-entangled state $|\mathcal{LP}_{01}\rangle_s |\mathcal{LP}_{11a}\rangle_i + e^{i\phi} |\mathcal{LP}_{11a}\rangle_s |\mathcal{LP}_{01}\rangle_i$, where phase ϕ can be changed by varying the pump phase difference $\Delta\phi = (\phi_{p1} + \phi_{p2}) - (\phi_{p3} + \phi_{p4})$. For each of the two processes in Fig. 1a, the phase-matching condition [8] requires equal group velocities at the average frequencies of the two waves in each spatial mode. These average frequencies, converted to wavelengths, are shown by dashed lines in Fig. 1a. Figure 1b shows measured relative inverse group velocities (RIGV) $1/\nu_g$ of LP_{01} , LP_{11a} , and LP_{11b} modes of our TMF. The LP_{11a} curve is approximately parallel to the LP_{01} curve and horizontally shifted from it by ~ 24 nm ($\Delta\nu_1 = 3$ THz), i.e., the phase matching is satisfied when the dashed lines in Fig. 1a are separated by 24 nm. Energy conservation and momentum conservation (phase matching) impose 4 constraints on the frequencies of the 6 involved waves: $\nu_{p1(p3)} = \nu_{i(s)} + \Delta\nu_1$ and $\nu_{p2(p4)} = \nu_{s(i)} - \Delta\nu_1$, hence any two frequencies that are not separated by $\Delta\nu_1$ can be arbitrarily chosen. In our experiment, we choose signal to be at 1571.9 nm and idler at 1561.5 nm, which results in pumps 1, 2, 3, and 4 placed at 1537.3, 1596.8, 1547.3, and 1586.2 nm, respectively.

II. EXPERIMENT

Our experimental setup is shown in Fig. 1c. The pumps 1–4 and signal are carved into 10-ns-long flat-top pulses with a 10-MHz repetition rate by 3 intensity modulators. The pumps are amplified by telecom-grade C- and L-band erbium-doped fiber amplifiers (EDFAs). Amplified pumps 1 and 3 are combined by a 50/50 coupler. Amplified pumps 2 and 4 are combined by a WDM coupler, converted to LP_{11a} mode by a phase plate (PP2), combined with the signal by a free-space beam splitter (BS1) and with pumps 1 and 3 by a free-space dichroic beam splitter (DBS), and then coupled into the 1-km-long TMF by an objective. TMF output is collimated by a second objective. We split the output between

an infrared camera and a single-mode fiber (SMF) connected to the optical spectrum analyzer (OSA), which in this case measures the LP_{01} “output port” of the TMF. By inserting phase plate PP3 prior to the OSA’s SMF input, we can also measure LP_{11a} “output port” of the TMF. We can gradually vary the signal spatial mode from LP_{01} to LP_{11a} by vertically moving the phase plate PP1 (when it is centered on the beam, it generates LP_{11a} mode; when it is far off the center, it leaves the mode in LP_{01} ; in the intermediate positions it generates various two-mode superpositions). To maximize IM-FWM, we co-polarize all three input waves in each process. Mode selectivity of each process separately is investigated by comparing the idler generated by the “correct” signal mode (LP_{01} for process 1, LP_{11a} for process 2) to that generated by the “wrong” mode (LP_{11a} and LP_{01} , respectively). As shown by black and purple traces in Fig. 2a, process 1 has better than 19 dB selectivity, and selectivity of process 2 is similar (not shown in Fig. 2a). Figure 2a also shows spectra when all 4 pumps are present, i.e., both processes 1 and 2 taking place simultaneously: LP_{01} port (red) and LP_{11a} port (blue) for signal in LP_{11a} mode. As expected, virtually no idler is present at the LP_{11a} port for such signal input.

With all 4 pumps present, Figure 2b shows the idler powers at the LP_{01} and LP_{11a} output ports for various two-mode input signal superpositions. Average powers inside the TMF are 0 dBm for the signal and 20, 7.5, 20, and 9 dBm for pumps 1, 2, 3, and 4, respectively. The pump powers are chosen to equalize the signal-to-idler conversion efficiencies (CEs) at -43 dB for processes 1 and 2. $CE = g - 1 = \langle n \rangle$, where g is the parametric gain, and $\langle n \rangle$ is the average number of generated photons per mode, also equal to the probability of a single pair generation for $CE \ll 1$ (our case). Figure 2b shows that, as the weight of LP_{11a} signal mode in the superposition changes from 0 to 100%, the total idler power remains constant (within 1 dB), while the weights of idler modes LP_{01} and LP_{11a} change from 0 to 100% and from 100% to 0, respectively, as expected for the generated idler mode that is orthogonal to the input signal mode. We are currently working on a stabilization scheme for phase $\Delta\phi = (\phi_{p1} + \phi_{p2}) - (\phi_{p3} + \phi_{p4})$, which would allow us to set the relative phase of the idler mode superposition to make it perfectly orthogonal to the signal mode superposition.

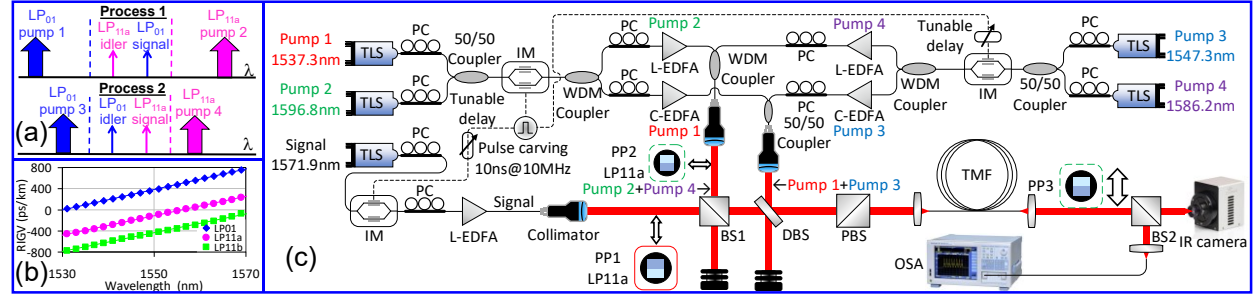


Fig. 1. (a) Two parametric processes, whose combination enables generation of spatial-mode-entangled signal-idler photon pairs in the TMF. (b) Measured relative inverse group velocity (RIGV) data for the modes of our TMF. (c) Experimental setup.

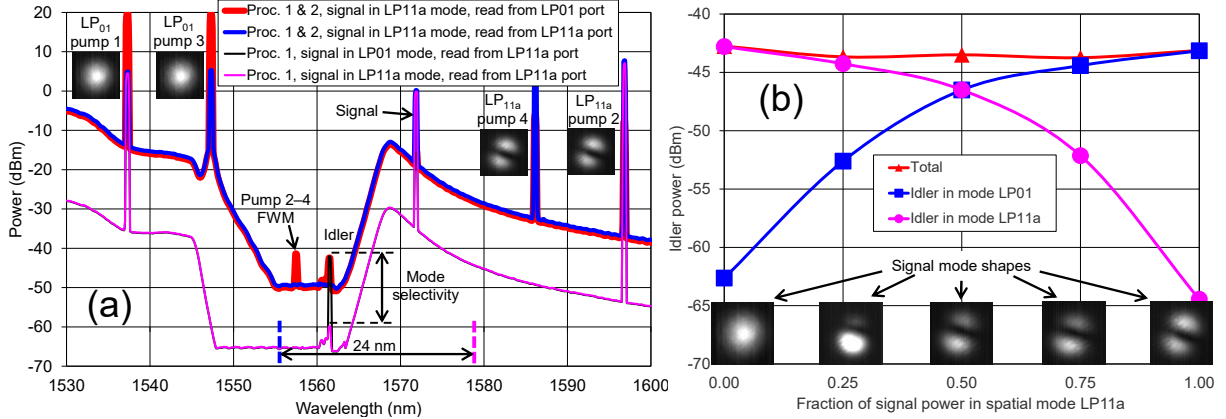


Fig. 2. (a) Spectra for process 1 alone (black, purple) and processes 1, 2 combined (red, blue). (b) Idler powers for various signal mode superpositions.

III. DISCUSSION AND CONCLUSIONS

We have demonstrated that a combination of two IM-FWM processes can couple arbitrary two-mode signal combination to an orthogonal idler mode. The next step, apart from phase stabilization, will be to observe this mode anticorrelation in single-photon regime, which will require drastic suppression of pump ASE, as well as narrow-band signal and idler filtering [9] and, perhaps, cooling of the fiber to suppress Raman noise.

This work has been supported in part by the NSF grants ECCS-1937860 and ECCS-1842680.

REFERENCES

- [1] W. Löffler *et al*, PRL **106**, 240505 (2011).
- [2] Y. Kang *et al*, PRL **109**, 020502 (2012).
- [3] D. Cozzolino *et al*, Adv Phot **1**, 046005 (2019).
- [4] K. Rottwitt *et al*, Fibers **6**, 32 (2018).
- [5] C. Guo *et al*, Opt Lett **44**, 235 (2019).
- [6] A. Shamshooli *et al*, CLEO 2020, JTh2A.29.
- [7] F. Parmigiani *et al*, OE **25**, 33602 (2017).
- [8] R.-J. Essiambre *et al*, PTL **25**, 539 (2013).
- [9] Y. B. Kwon *et al*, CLEO 2017, FF2E.1.